© 2025 Journal of Pharmacy & Pharmacognosy Research, 13 (s1), S27-S46, 2025
ISSN 0719-4250
https://jppres.com

DOI: https://doi.org/10.56499/jppres24.2109_13.s1.27

Original Article

Isolation and characterization of fatty acid esters from *Cyperus marginatus* Thunb. leaf, their *in vitro* biological and *in silico* molecular docking studies

[Aislamiento y caracterización de ésteres de ácidos grasos de hojas de *Cyperus marginatus* Thunb., estudios de acoplamiento molecular *in silico* y biológico *in vitro*]

Gugulethu M. Miya[1], Ayodeji O. Oriola[1*], Pallab Kar[2], Adebola O. Oyedeji[1,2***]**

[1]Department of Chemical and Physical Sciences, Walter Sisulu University, Nelson Mandela Drive, P/Bag X1, Mthatha 5117, South Africa.
[2]African Medicinal Flora and Fauna Research Niche, Walter Sisulu University, Nelson Mandela Drive, P/Bag X1, Mthatha 5117, South Africa.
E-mail: *aooriola@gmail.com; **pallabkar.bio@gmail.com; ***aoyedeji@wsu.ac.za

Abstract

Context: Fatty acid esters (FAEs) are a unique class of secondary metabolites with promising antioxidant and anti-inflammatory properties, making them useful ingredients for cosmetic formulations. So far, many plants in the *Cyperus* genus (family *Cyperaceae*) are known to contain FAEs, among other classes of phytochemicals. However, *Cyperus marginatus* (CM) is one of the under-investigated species in this genus.

Aims: To evaluate CM for its antioxidant (AOX) and anti-inflammatory FAEs.

Methods: Two FAEs were isolated from CM leaf dichloromethane extract by silica gel column chromatography, while compound characterization was based on organic spectroscopy (NMR and MS). The antioxidant evaluation was by *in vitro* inhibitory effects against the 2,2-diphenyl-1-picrylhydrazyl (DPPH), nitric oxide (NO), and ferric ion (Fe^{3+}) radicals, while anti-inflammatory activity was based on the egg albumin denaturation (EAD) assay. The FAEs were molecularly docked against NADPH oxidase 2 (NOX2) and nuclear factor (NF-κB).

Results: The isolated FAEs were elucidated as ethyl margarate, and a newly described FAE, nonadecanoic acid-2-ethoxy ethyl ester. Ethyl margarate demonstrated better AOX properties, with lower inhibition against DPPH (IC_{50} = 43.82 ± 1.44 µg/mL), NO (60.04 ± 3.28 µg/mL), and Fe^{3+} (308.01 ± 34.11 µgAAE/mg) radicals. It also demonstrated a better anti-inflammatory response with an IC_{50} of 12.24 ± 0.69 µg/mL against EAD, which was comparable to diclofenac (IC_{50} = 11.94 ± 1.37 µg/mL). Molecular docking studies revealed the significant binding affinities of ethyl margarate to NOX2 and NF-κB at -7.2 and -6.1 kcal/mol, respectively.

Conclusions: Ethyl margarate isolated from *C. marginatus* has been shown through this study to be a promising antioxidant and anti-inflammatory FAE.

Keywords: anti-inflammatory; antioxidant; *Cyperus marginatus*; ethyl margarate; fatty acid esters.

Resumen

Contexto: Los ésteres de ácidos grasos (FAE) son una clase única de metabolitos secundarios con prometedoras propiedades antioxidantes y anti-inflamatorias, lo que los convierte en ingredientes útiles para formulaciones cosméticas. Hasta ahora, se sabe que muchas plantas del género *Cyperus* (familia *Cyperaceae*) contienen FAE, entre otras clases de fitoquímicos. Sin embargo, *Cyperus marginatus* (CM) es una de las especies menos investigadas de este género.

Objetivos: Evaluar CM por sus FAE antioxidantes (AOX) y anti-inflamatorios.

Métodos: Se aislaron dos FAE del extracto de diclorometano de hojas de CM mediante cromatografía en columna de gel de sílice, mientras que la caracterización del compuesto se basó en espectroscopia orgánica (RMN y EM). La evaluación antioxidante se realizó mediante efectos inhibidores *in vitro* contra los radicales 2,2-difenil-1-picrilhidrazilo (DPPH), óxido nítrico (NO) e ión férrico (Fe^{3+}), mientras que la actividad anti-inflamatoria se basó en el ensayo de desnaturalización de albúmina de huevo (EAD). Los FAE se acoplaron molecularmente contra la NADPH oxidasa 2 (NOX2) y el factor nuclear (NF-κB).

Resultados: Los FAE aislados se dilucidaron como margarato de etilo y un FAE recién descrito, el éster etílico del ácido nonadecanoico-2-etoxietil. El margarato de etilo demostró mejores propiedades AOX, con menor inhibición contra los radicales DPPH (IC_{50} = 43,82 ± 1,44 µg/mL), NO (60,04 ± 3,28 µg/mL) y Fe3+ (308,01 ± 34,11 µgAAE/mg). También demostró una mejor respuesta anti-inflamatoria con una CI_{50} de 12,24 ± 0,69 µg/mL contra EAD, que fue comparable al diclofenaco (CI_{50} = 11,94 ± 1,37 µg/mL). Los estudios de acoplamiento molecular revelaron las afinidades de unión significativas del margarato de etilo a NOX2 y NF-κB a -7,2 y -6,1 kcal/mol, respectivamente.

Conclusiones: Se ha demostrado a través de este estudio que el margarato de etilo aislado de *C. marginatus* es un prometedor antioxidante y FAE anti-inflamatorio.

Palabras Clave: anti-inflamatorio; antioxidante; *Cyperus marginatus*; ésteres de ácidos grasos; margarato de etilo.

ARTICLE INFO
Received: June 1, 2024.
Accepted: January 29, 2025.
Available Online: February 21, 2025.

AUTHOR INFO
ORCID:
0000-0002-3314-5391 (GMM)
0000-0002-2340-3174 (PK)
0000-0002-4166-0449 (AOOr)
0000-0001-8765-7766 (AOOy)

INTRODUCTION

Fatty acid esters (FAEs) are a unique and common component of lipids. They vary in their chain length (hydrocarbon tail), number and position of double bonds, and pattern of substitution of their carboxylic head (Burdge and Calder, 2015). They are naturally abundant in many plant families, such as *Fabaceae*, *Lauraceae*, *Cucurbitaceae*, *Lamiaceae*, *Poaceae*, and *Cyperaceae* (Li et al., 2017). Chemically, nonadecanoic acid ethyl ester, ethyl stearate, and myristic, lauric, oleic, palmitic, linoleic, α-linolenic, 8-octadecenoic, behenic, undecylic, arachidic and hexadecatrienoic acids, are among the FAEs identified in many sedges (*Cyperus*) (Miya et al., 2023; Oderinde and Tairu, 1988; Rivera et al., 2015; Slobodianiuk et al., 2021). These compounds are known to exhibit considerable biological properties, including antioxidant and anti-inflammatory activities (Lin et al., 2018), with some of them, notably lauric and stearic acid esters, utilized for cosmetic formulations (Goyal et al., 2022). Comprising over 700 species, the *Cyperus* genus is recognized as the second-largest genus within the *Cyperaceae* family. The genus is widely distributed globally, encompassing various regions, including South Africa (Gambo and Da'u, 2014; Sharma and Singh, 2011; Srivastava et al., 2014). *Cyperus marginatus* Thunberg species is widely distributed across Southern Africa, except Botswana (Browning et al., 1999). *C. marginatus* is a perennial herb, thriving in temporary wet habitats along the Northern Cape Province of South Africa (Malan, 2003). In the KwaZulu-Natal Province, however, they commonly establish their roots in shallow, persistently flowing water, often amidst rocky surroundings (Kotze and Traynor, 2011). A decoction of its roots is used in traditional medicine for the treatment of sore throat or mumps, the leaf sheath is a raw material for mat making, and the whole plant is traded as an ornamental pond plant in South Africa (Lall, 2020). Many species of *Cyperus*, including *C. esculentus*, *C. scariosus*, *C. rotundus* and *C. longus*, have been investigated for their putative bioactive compounds, including antioxidant and anti-inflammatory activities (Ait-Ouazzou et al., 2012; Al-Snafi, 2016; Gamal et al., 2015; Gugsa and Yaya, 2018; Kakarla et al., 2016; Kotze and Traynor, 2011; Sharma and Singh, 2011; Srivastava et al., 2014), to the best of our knowledge, *C. marginatus* has not been exploited in this regard. Therefore, this study reports the isolation and characterization of two FAEs from *C. marginatus* for the first time, while their antioxidant and anti-inflammatory activities were also determined *in vitro* and *in silico*.

MATERIAL AND METHODS

General experimental procedure

Reagents and solvents were of analytical grade and purchased from Sigma-Aldrich (Pty) Ltd., Johannesburg, South Africa. Silica gel for TLC and column chromatography was procured from Merck (Pty) Ltd., Johannesburg, South Africa. Absorbance was read on the 680-Bio-Rad microplate reader (Serial Number 14966, USA). Spectroscopic analysis of the isolated compounds was performed on a 400 MHz Varian NMR spectrometer and 600 MHz Bruker Biospin GmbH spectrometer (Agilent Technologies, USA) situated at Stellenbosch University, South Africa. Tetramethyl silane (TMS) was used as the NMR internal standard, while chemical shift (δ) was recorded in parts per million (ppm). The compounds were examined in deuterated benzene. The molecular mass of each compound was determined by the electron-spray-ionization method on a Waters API Q-TOF Ultima mass spectrometer (Waters Corporation, Manchester, UK), also located at Stellenbosch University, South Africa. The mass-to-charge ratio of each fragment was recorded in m/z at a scan range of m/z 100-1000.

Plant material

All experimental methods, including plant collection, were carried out in accordance with the IUCN policy and other relevant guidelines (Dudley, 2008). The study, including the collection of plant material, was granted academic permission by the Chairperson, Faculty of Natural Sciences Graduate Research Ethics Committee, Walter Sisulu University (WSU), with an approval reference number WSU/FNS-GREC-2021/02-22/G2. Permission was granted by Botanica Natural Products, Alldays (latitude: -22.6823° S, longitude: 29.1012° E), Limpopo Province, South Africa, for collection of the fresh leaves of *Cyperus marginatus* after submitting the institutional study approval. The plant was identified by Mr. Will Coetsee, the curator of the botanical garden. Thereafter, a herbarium specimen of the plant was deposited in the University of Pretoria Herbarium Unit, with voucher number MGM 007. The leaves were air-dried at room temperature (≈25°C) and milled into powder for further work.

Sequential solvent extraction

The powdered leaves of CM were sequentially extracted in increasing levels of polarity from n-hexane (Hex) to ethanol (EtOH). In detail, 786 g of CM was exhaustively extracted with 7.5 L of Hex, filtered, and

concentrated to dryness in vacuo. The marc was subsequently extracted with 6.5 L of dichloromethane (DCM), 7.5 L of ethyl acetate (EtOAc), and 5.5 L of EtOH, respectively, thus affording the gradient extracts.

Fractionation of DCM crude extract

An amount of 22.8 g of the DCM extract was solubilized in 50 mL of acetone, adsorbed unto 60 g silica gel, and dry-packed on a 200 g silica gel glass column of 600 × 50 mm dimension (L × i.d). The adsorbed extract was eluted with 600 mL each solvent systems in increasing level of polarity, Hex (100%), Hex-DCM (90:10, 80:20, 70:30, 60:40, 50:50, 40:60, 30:70, 20:80, 10:90%), DCM (100%), DCM-EtOAc (90:10, 80:20, 70:30, 60:40, 50:50, 40:60, 30:70, 20:80, 10:90%), EtOAc (100%), EtOAc-MeOH (90:10, 80:20, 50:50%) and MeOH (100%). The elution process afforded 121 column fractions.

TLC bioautography of DCM chromatographic fractions

The DCM chromatographic eluates were analyzed for their bioactive fatty acid compounds using the method described by Oriola et al. (2021) with slight modification. Fractions were spotted in two replicates on a silica gel TLC plate. Each plate was developed in 50 mL of Hex-DCM-acetic acid (8:1.5:0.5) trinary solvent system to resolve the FAEs (Esperón-Rojas et al., 2018). One replicate of the TLC chromatogram was sprayed with 10% sulfuric acid, while the other was sprayed with 0.5 mg/mL DPPH in MeOH solution to identify the free radical scavenging (potentially bioactive) spots. The eluates were bulked into 21 subfractions, F1-F21.

Antioxidant tests

DPPH spectrophotometric assay

This procedure was conducted following a previously established method (Ayodele et al., 2024) with certain adaptations. In this process, 0.5 mL of 0.1 mM DPPH radical in methanol was introduced to 0.5 mL of serially diluted isolated compounds and L-ascorbic acid within a concentration range of 100.00, 50.00, 25.00, 12.50, and 6.25 µg/mL, each in triplicate. The resulting mixture underwent incubation in the dark at 37°C for 30 min. Subsequently, absorbance was measured at 515 nm using a microplate reader at the starting absorbance of DPPH ~0.655. The percentage inhibition of the radical was calculated according to Equation [1].

$$\text{Inhibition (\%)} = \frac{(\text{ABScontrol} - \text{ABSsample})}{(\text{ABScontrol})} \times 100 \quad [1]$$

Where ABSsample: Absorbance of the test sample (n = 3), while ABScontrol: Absorbance of negative control (n = 3) (methanol).

Nitric oxide (NO) inhibition assay

The inhibitory impact of the isolates on the NO radical was assessed following the approach outlined by Sarker et al. (2022) with modifications. Nonadecanoic acid and ethyl margarate (heptadecanoic ethyl ester) were prepared at various concentrations ranging from 100.00 to 6.25 µg/mL. These preparations were then added to 0.2 mM (2 mL) of sodium nitroprusside in triplicates. The resulting reaction mixture underwent incubation at 25°C for 3 h, after which 0.5 mL of the mixture was combined with Griess reagent (0.33% sulphanilamide dissolved in 20% glacial acetic acid and mixed with 1 mL of naphthylethylenediamine chloride at 0.1% w/v). The complex and Griess reagent mixture was left to incubate at room temperature for 30 min, followed by the immediate measurement of absorbance at 540 nm using a microplate reader. The percentage inhibition of the radical was calculated according to Equation [1].

Ferric reducing antioxidant power (FRAP) assay

The assessment of the reducing antioxidant capacity of nonadecanoic acid and ethyl margarate (heptadecanoic ethyl ester) followed the procedure outlined (Miya et al., 2023), with certain adaptations. The isolates were dissolved in methanol and introduced into a mixture containing 0.25 mL of phosphate buffer (0.2 M; pH 6.6) and 0.25 mL of potassium ferricyanide [$K_3Fe(CN)_6$] (1% w/v). (1% w/v). L-ascorbic acid served as the standard compound. After incubation at 50°C for 20 min, 0.25 mL of CCl_3COOH (10% w/v) was added, followed by centrifugation at 3000 rpm for 10 minutes. The upper layer of the solution was combined with 1 mL of methanol and an equal amount of 0.5 mL of $FeCl_3$ (0.1%, w/v). Conducted in triplicate, the experiment's absorbance was measured at 700 nm on a microplate reader against a blank sample containing only phosphate buffer. The ferric reducing power of the isolates at concentrations of 100.00, 50.00, 25.00, 12.50, and 6.25 µg/mL in methanol was determined as ascorbic acid equivalent (AAE) using the calibration curve of the positive control (L-ascorbic acid).

Protein (egg albumin) denaturation assay

The *in vitro* anti-inflammatory response of the isolated compounds to act against protein denaturation was determined using the egg albumin denaturation (EAD) assay (Oriola et al., 2023). A reaction mixture comprising 0.2 mL of albumin content of fresh chicken egg, 2.8 mL of phosphate buffer saline at pH 6.4, and 2 mL each of the isolated compounds and diclo-

fenac (standard drug) at 100, 50, 25, 12.5, 6.25 and 3.125 µg/mL concentrations was prepared in triplicate. The reaction mixture was incubated at 37°C for 15 min away from direct light and thereafter boiled at 70°C for 5 min in a thermostatic water bath. The resulting mixture was cooled, and the absorbance was measured at 655 nm. The percentage inhibition of EAD was determined according to Equation [2].

$$\text{Inhibition of EAD (\%)} = \frac{(\text{ABScontrol} - \text{ABSsample})}{(\text{ABScontrol})} \times 100 \quad [2]$$

Where ABScontrol: Absorbance of negative control (n = 3), ABSsample: Absorbance of sample (n = 3).

In silico molecular docking

Preparation and refinement of the protein and ligand structures

The molecular docking investigation was carried out to target proteins associated with oxidative stress and inflammation. In this instance, the proteins of choice are NOX2 and NF-κB. The PDB structure of NOX2 and NF-κB with PDB Ids 7U8G (Noreng et al., 2022) and 4DN5 (Liu et al., 2012) was acquired from the Protein Data Bank (http://www.rcsb.org). To prepare the protein structures for docking, polar hydrogen atoms and Kollman charges were added after removing water atoms using AutoDockTools.

The concerned phytocompounds were downloaded from the NCBI PubChem (https://pubchem.ncbi.nlm.nih.gov/). The Open Babel Server was then used to transform the downloaded sdf structures into pdb structures (O'Boyle et al., 2011). The ligand structures underwent energy minimization using the Gromos 96 force field after the PRODRG server (Schüttelkopf and van Aalten, 2004) was used to optimize their energy.

Determination of active sit and molecular docking

The active site of the proteins (NOX2, and NF-κB) was predicted using the literature (Liu et al., 2012; Noreng et al., 2022) and validated through the CASTp 3.0 (Computed Atlas of Surface Topography of Proteins) online server (Binkowski et al., 2003). The processed protein without a native inhibitor was uploaded to the CASTp 3.0 server and the top result from the best three potential ligand-binding sites was chosen for docking. The amino acid residues predicted by CASTp 3.0 were then compared with the amino acids in the active site of the native inhibitor-NOX2 co-crystallized complex, and native inhibitor-NF-κB co-crystallized complex. This was done by manually opening the co-crystallized complex in the Discovery studio visualization tool (Kar et al., 2022a) to verify the active site. This allowed for the identification of the interacting residues, which were found to be quite similar to those predicted by the CASTp 3.0 server. The Autodock and Autogrid tools integrated with Autodock4 were used to generate grid maps (X; Y; and Z confirmations; Box center and Box dimension) for each atom of the native inhibitor ligand. In order to obtain the X; Y; and Z confirmations (Box center and Box dimension) as a potential target site, molecular docking was carried out using the Autodock4 (Naidoo et al., 2021; Trott and Olson, 2010). Using a grid-based docking technique, the ligands of interest were molecularly docked in the active binding sites of the relevant proteins using a stiff protein receptor and a flexible ligand docking methodology (Kar et al., 2021; 2022a; 2022b). A grid box involving the active site residues of the NOX2 protein was created, with center_x = 144.17, center_y = 141.08, center_z = 151.25, size_x = 27.0, size_y = 34.0, and size_z = 35.0. Similarly, a grid box covering the active binding pocket of NF-κB was employed, with center_x= -8.0, center_y= 30.1, center_z= -4.6, size_x= 24.0, size_y= 15.1, and size_z= 18.9. After Autodock Vina finished the molecular docking procedure, the docked complexes were visualized using the Discovery Studio visualization tool (Kar et al., 2022a; 2022b).

Assessment of physicochemical features and potential toxicity of the phytocompounds

For additional physicochemical properties and drug-like feature evaluation, the phytocompounds with the corresponding proteins in AutoDock Vina were selected (Naidoo et al., 2021). The SwissADME server was utilized to estimate the physicochemical parameters, and the pkCSM server was used for validation (Daina et al., 2017; Pires et al., 2015). The compounds' potential toxicity (cytotoxicity, carcinogenicity, hepatotoxicity, mutagenicity (AMES mutagenesis), and P-glycoprotein inhibitor) were evaluated using the ProTox-II and vNN-ADMET online servers (Banerjee et al., 2018; Schyman et al., 2017).

Molecular dynamics simulations

A critical step in validating molecular docking data is molecular dynamics simulation (MDS), which provides an accurate assessment of the potential stability of protein-ligand complexes (Kar et al., 2021). Using the GROMACS (version 2019) force field parameters (GROMOS96 43a1), the compounds were exposed to MDS for 120 ns (Abraham et al., 2015; Kar et al., 2021; 2022a; 2022b). The equilibration stages were determined using the constant pressure and temperature (NPT) ensemble (Elfiky and Azzam, 2021; Enayatkhani et al., 2021; Umesh et al., 2021). Umesh et al. (2021) state that the MD simulations were performed at a standard pressure of 1.013 bar

and standard temperature of 300 K. Using the root-mean-square-deviation/fluctuation (RMSD/F) analysis, an assessment of the complexes' structural and conformational stability was found.

Statistical analysis

Statistical analysis data are expressed as mean ± SEM (n = 3); data subjected to statistical analysis by One-way ANOVA with different alphabets in superscript considered significant at $p<0.05$, utilizing the Excel statistical application (Microsoft 365, Microsoft Corporation, USA).

RESULTS AND DISCUSSION

TLC bioautography of DCM chromatographic fractions

The DCM fraction upon chromatographic fractionation afforded subfractions F1 and F2, both faintly yellowish with whitish deposits. TLC analysis of the fractions revealed faintly yellowish spots, which turned brownish with 10% sulfuric acid spray. They also bleached the purple DPPH radical solution, thus indicating the presence of FAEs with strong radical scavenging properties. Sub-fractions F1 and F2 were washed in 50 mL each of Hex (100%), affording compounds CM-1 and CM-2 [faintly brownish spots, R_f 0.73 and 0.69, respectively in Hex-DCM-acetic acid (8:1.5:0.5)].

Characterization of isolated compounds

Spectroscopic data of CM-1

^{1}H NMR (400 MHz in C_6D_6), δ ppm: 0.88 (H, t, 0.88 (3H, *t*, *J*=7.2 Hz, H-17), 1.25 (3H, H-2′), 2.28 (2H, *t*, *J*=7.6, 6.8 Hz, H-2), 4.05 (2H, *q*, *J*=6.8, 6.8 Hz, H-1′); ^{13}C NMR (150 MHz in C6D6), δ ppm: 173.96 (C-1), 64.31 (C-1′), 34.40 (C-2), 31.91 (C-15), 29.14 (C-6), 29.26 (C-7), 29.35 (C-8), 29.47 (C-9), 29.52 (C-10), 29.57 (C-11), 29.59 (C-12), 29.65 (C-13), 29.69 (C-14), 28.63 (C-5), 25.92 (C-4), 25.02 (C-3), 22.68 (C-16), 14.11 (C-17, C-2′). The LC-MS/MS chromatograms of the isolated compound and the full NMR data are indicated as supplementary data Figs. S1–S3.

Spectroscopic data of CM-2

^{1}H NMR (600 MHz in C_6D_6), δ ppm: 0.91 (3H, *t*, *J*=6.0 Hz, H-19), 1.19 (3H, *t*, *J*=6.6 Hz, H-4′), 2.21 (2H, *t*, *J*=7.4 Hz, H-2), 3.38 (2H, *t*, *J*=6.4 Hz, H-3′), 4.08 (2H, *t*, *J*=12.0 Hz, H-2′), 4.24 (2H, *t*, *J*=6.5 Hz, H-1′); ^{13}C NMR (150 MHz in C_6D_6), δ ppm: 172.75 (C-1), 64.31 (C-1′), 34.60 (C-2), 32.35 (C-16), 30.20 (C-15), 30.14 (C-13), 30.08 (C-14), 30.05 (C-11), 29.99 (C-12), 29.94 (C-9), 29.80 (C-10), 29.73 (C-8), 29.69 (C-7), 29.59 (C-6), 29.26 (C-5), 26.41 (C-4), 25.49 (C-3), 23.10 (C-17), 14.29 (C-18, C-2′); TOF ES$^+$/MS (% rel. abundance): *m/z* 371.3010 (21.5%) [M+H]$^+$, m/z 304.2997 (80.0%) [M-65]$^+$. The LC-MS/MS chromatograms of the isolated compound and the full NMR data are indicated as supplementary data Figs. S4–S6.

Structure elucidation of characterized compounds

Ethyl margarate (CM-1)

Based on NMR analysis (Table 1 and supplementary data Figs. S1–S3), CM-1 showed a shielded triplet signal at 0.88 ppm, which is indicative of a terminal methyl group. The quartet signal at 4.05 ppm suggests the presence of an oxygenated methylene proton that is directly attached to a methyl group, suggesting an ethyl ester moiety. Also, the presence of a triplet signal at 2.28 ppm represents the first methylene proton that is next to the carbonyl ester functional group. The carbonyl ester was further substantiated in the ^{13}C NMR, with a downfield resonance at 173.9 ppm, while also showing a total of nineteen signals, representing nineteen carbon atoms. The existence of nine overlapping signals around 29 ppm suggested the presence of nine chemically equivalent methylene carbons. Upon comparison of the spectra data of CM-1 with that of ethyl heptadecanoate reported in the seeds of *Aesculus indica* (Yadav et al., 2022), as presented in Table 1, the compound was characterized as heptadecanoic acid ethyl ester, also known as ethyl margarate (Fig. 1A), which is reported for the first time from *C. marginatus*.

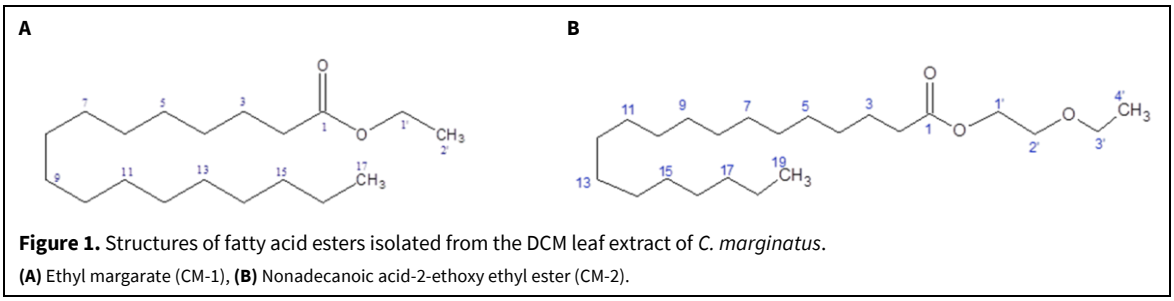


Figure 1. Structures of fatty acid esters isolated from the DCM leaf extract of *C. marginatus*.
(A) Ethyl margarate (CM-1), **(B)** Nonadecanoic acid-2-ethoxy ethyl ester (CM-2).

Table 1. The observed ^{1}H- and ^{13}C NMR spectra data assignment of isolated ethyl margarate (CM-1).

Position	Type of carbon	^{1}H NMR (multiplicity, J)	^{13}C NMR	Ethyl heptadecanoate (Yadav et al., 2022)	
				^{1}H NMR (multiplicity, J)	^{13}C NMR
1	C=O, ester	-	173.9	-	173.5
	O-$\underline{CH_2}$	4.05 (*q*, *J*=6.8 Hz)	64.4	4.01 (*q*, *J*=6.0 Hz)	59.6
	CH_3	1.25	14.1	1.25 (*t*, *J*=6.0 Hz)	13.9
2	CH_2	2.28 (*t*, *J*=7.2 Hz)	34.4	2.28 (*t*, *J*=8.05 Hz)	33.7
3	CH_2	1.61 (*m*)	25.0	1.61 (*m*)	24.7
4	CH_2	1.25 (*m*)	25.9	1.25 (*m*)	28.9
5	CH_2	1.25 (*m*)	28.6		29.8
6	CH_2	1.25 (*m*)	29.1		29.0
7	CH_2	1.25 (*m*)	29.3		29.2
8	CH_2	1.25 (*m*)	29.4		29.4
9	CH_2	1.25 (*m*)	29.5	1.25 (*m*)	29.4
10	CH_2	1.25 (*m*)	29.5		29.4
11	CH_2	1.25 (*m*)	29.6	1.25 (*m*)	29.4
12	CH_2	1.25 (*m*)	29.6	1.25 (*m*)	29.4
13	CH_2	1.25 (*m*)	29.7	1.25 (*m*)	29.1
14	CH_2	1.25 (*m*)	29.7	1.25 (*m*)	29.9
15	CH_2	1.25 (*m*)	31.9	1.25 (*m*)	31.7
16	CH_2	1.25 (*m*)	22.7	1.28 (*m*)	22.4
17	CH_3	0.88 (*t*, *J*=7.2, 6.4 Hz)	14.1	0.80 (*t*, *J*=6.0 Hz)	12.7

d: doublet; *dd:* doublet of a doublet; *t:* triplet; *m:* multiplet; CH3: methyl; CH_2: methylene; CH: methine; *J:* coupling constant is expressed in Hertz (Hz).

Nonadecanoic acid-2-ethoxy ethyl ester (CM-2)

As presented in Table 2 and supplementary data Figs. S4–S6, the ^{1}H NMR of CM-2 exhibited a triplet signal at 0.91 ppm, indicating the presence of a terminal methyl group. Three oxygenated methylene protons were identified at 3.38, 4.08, and 4.24 ppm. These signals corresponded to 62.8, 64.3, and 64.9 ppm in the ^{13}C NMR, which is indicative of an ethoxy-ethyl ester moiety (Pavia et al., 2013). The triplet signal at 14.3 ppm indicates the methyl group, the overlapping signals at 29-30 ppm indicate the aliphatic hydrocarbon chain, while the most deshielded signal at 172.8 ppm represents a carbonyl functional group of an ester. The similarities in the NMR data of CM-2 to that of Nonadecanoic acid (Yoo et al., 2002) assisted with the elucidation of the compound as a fatty acid ester. The full assignment of the NMR data of CM-2 is presented in Table 2. Thus, CM-2 is newly described in this study as nonadecanoic acid-2-ethoxy ethyl ester (Fig. 1B).

In vitro antioxidant assay

The biological activities of the isolated FAEs were evaluated based on their capacity to inhibit free radical actions of DPPH (Fig. 2) and nitric oxide (NO) (Fig. 3), as well as their ability to reduce ferric ion (Fe^{3+}) to ferrous ion (Fe^{2+}) *in vitro*, as detailed in Table 3. The results demonstrated that Ethyl margarate (CM-1) exhibited superior antioxidant properties among the isolated compounds, with an IC_{50} of 43.82 ± 1.44 µg/mL against the DPPH radical, 60.04 ± 3.28 µg/mL against NO, and 308.01 ± 34.11 µgAAE/mg against Fe^{2+} radicals. Notably, ethyl margarate (CM-1) displayed approximately one-third of the antioxidant capacity (FRAP) compared to L-ascorbic acid, the standard antioxidant compound. The presence of an alkoxy group, such as the ethoxy side-chain identified in CM-2, has been reported to cause a marked reduction in the antioxidant activity of an entire molecule (Platzer et al., 2022). Thus, this may justify the lower antioxidant activity of CM-2 compared to CM-1 in this study. Medium fatty acid esters have been recognized for their thickening agent, emollient, and lubricant activities (Vadgama et al., 2015). Conversely,

Table 2. The observed ^{1}H- and ^{13}C NMR spectra data assignment of isolated nonadecanoic acid-2-ethoxy ethyl ester (CM-2).

Position	Type of carbon	^{1}H NMR (multiplicity, J)	^{13}C NMR	Nonadecanoic acid ethyl ester (Yoo et al., 2002) ^{13}C NMR
1	C=O, ester	-	172.8	173.0
	O-$\underline{CH_2}$	4.24 (*t*, *J*=6.5 Hz)	64.9	
	$\underline{CH_2}$-O	4.08 (*t*, *J*=12.0 Hz)	64.3	64.3
	O-$\underline{CH_2}$	3.38 (*t*, *J*=6.4 Hz)	62.8	
	CH_3	1.19 (*t*, *J*=6.6 Hz)	14.3	14.3
2	CH_2	2.21 (*t*, *J*=7.4 Hz)	34.6	34.6
3	CH_2	1.50-1.55 (*m*)	25.5	25.5
4	CH_2	1.21-1.27 (*m*)	26.4	26.4
5	CH_2	1.21-1.27 (*m*)	29.3	29.3
6	CH_2	1.21-1.27 (*m*)	29.6	29.6
7	CH_2	1.21-1.27 (*m*)	29.7	29.7
8	CH_2	1.21-1.27 (*m*)	29.7	29.7
9	CH_2	1.21-1.27 (*m*)	29.9	29.9
10	CH_2	1.21-1.27 (*m*)	29.8	29.8
11	CH_2	1.21-1.27 (*m*)	30.1	30.1
12	CH_2	1.21-1.27 (*m*)	29.9	30.0
13	CH_2	1.21-1.27 (*m*)	30.1	30.1
14	CH_2	1.21-1.27 (*m*)	30.6	30.1
15	CH_2	1.21-1.27 (*m*)	30.2	30.2
16	CH_2	1.21-1.27 (*m*)	31.5	30.2
17	CH_2	1.21-1.27 (*m*)	32.4	32.4
18	CH_2	1.36 (*m*)	23.1	23.1
19	CH_3	0.91 (*t*, *J*=6.0 Hz)	14.3	14.3

d: doublet; *t*: triplet; *m*: multiplet; CH_3: methyl; CH_2: methylene; *J*: coupling constant is expressed in Hertz (Hz).

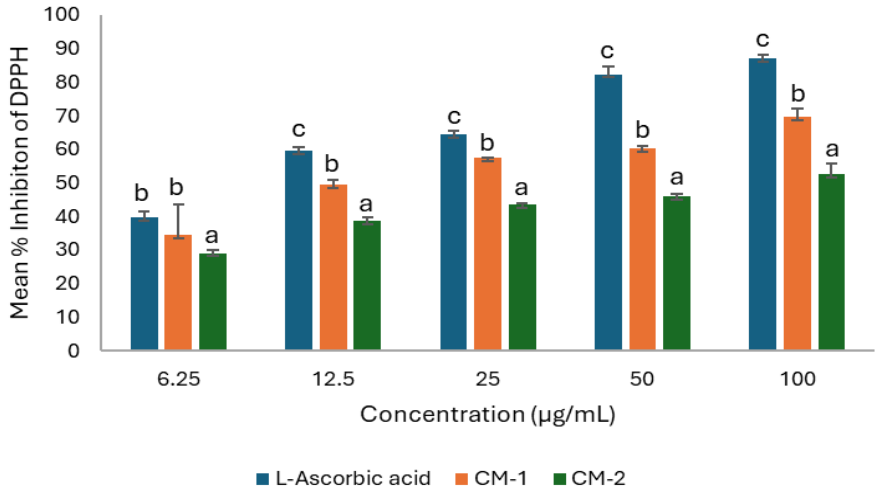


Figure 2. DPPH radical scavenging activities of fatty acid esters isolated from the DCM extract of *C. marginatus*.

CM-1: Ethyl margarate; CM-2: Nonadecanoic acid-2-ethoxy ethyl ester.

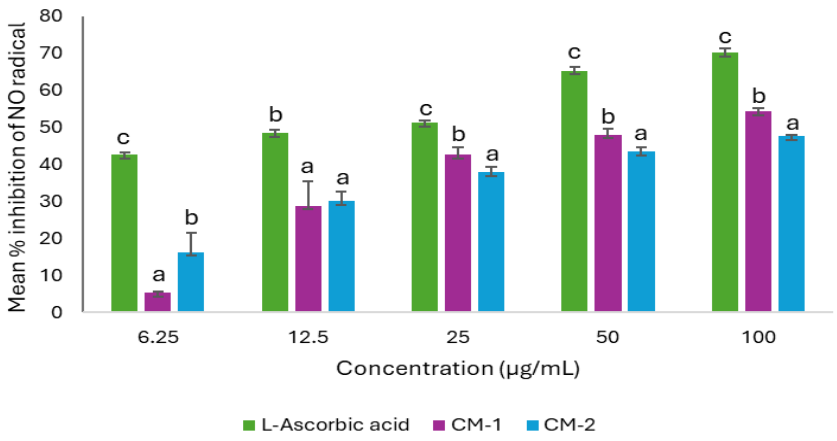


Figure 3. Nitric oxide inhibitory effects of fatty acid esters from the DCM extract of *C. marginatus*.
CM-1: Ethyl margarate; CM-2: Nonadecanoic acid-2-ethoxy ethyl ester.

Table 3. Antioxidant activities of fatty acid esters from the dichloromethane leaf extract of *C. marginatus*.

Isolated compound	DPPH (IC_{50} ± SEM) (µg/mL)	NO (IC_{50} ± SEM) (µg/mL)	FRAP (µgAAE/mg)
Ethyl margarate	43.82 ± 1.44^{b}	60.04 ± 3.28^{b}	308.01 ± 34.11^{bc}
Nonadecanoic acid-2-ethoxy ethyl ester	69.06 ± 5.10^{c}	76.65 ± 1.31^{e}	176.79 ± 11.83^{a}
L-ascorbic acid (standard)	8.92 ± 1.26^{a}	21.89 ± 1.32^{a}	N/A

Data are expressed as mean ± SEM (n = 3); data was subjected to statistical analysis by One-way ANOVA followed by the student *t*-test; data with different alphabets in superscript are considered significant at $p<0.05$. AAE: L-ascorbic acid equivalent; N/A: not applicable.

long fatty acid esters have demonstrated antibacterial, antioxidant, flavor-enhancing, and anti-inflammatory activities (Abubakar and Majinda, 2016; Aparna et al., 2012; Prematilaka and Silva, 2016). Numerous studies have highlighted the diverse biological properties of medium-to-long chain fatty acids and their esters, encompassing antioxidant, cytotoxic, anti-inflammatory, and anti-aging activities (Antwi et al., 2018; Dederen et al., 2012; Demirpolat et al., 2022; Han et al., 2014). In fact, stearic acid esters are currently utilized as significant ingredients in the formulation of skincare products within the pharmaceutical and cosmeceutical industries (Dharmadeva et al., 2018; Fiume et al., 2012). In summary, the compounds derived from *Cyperus marginatus* hold promise for contributing novel pharmaceutical and cosmeceutical agents that may be beneficial for inhibiting ROS-related disorders.

Evaluation of *in vitro* anti-inflammatory activity

The theory behind the egg albumin denaturation experiment is that compounds having anti-inflammatory properties should be able to stabilize protein structures and stop denaturation, which is commonly connected to tissue damage and inflammation. Therefore, phytocompounds that in this assay considerably reduce egg albumin's denaturation and may have anti-inflammatory effects (Prematilaka and Silva, 2016). One of the main causes of inflammation is protein denaturation and cellular infiltration, and leukocytes release lysosomal contents that include proteases and bactericidal enzymes that worsen tissue damage and the inflammatory response (Prematilaka and Silva, 2016). In this study, Fig. 4 displays the compounds' inhibitory effects on protein denaturation (egg albumin). According to Fig. 4, it was interesting to note that ethyl margarate (heptadecanoic acid ethyl ester) (CM-1) exhibited the highest percentage inhibition from 6.25 µg/mL concentration (69.11 ± 2.24%) up to 100 µg/mL concentration (87.30 ± 1.87%) whereas, at the lowest concentration (3.125 µg/mL), diclofenac showed the highest inhibition (21.69 ± 1.21%). Nonetheless, the summarized anti-inflammatory reaction (Table 4) showed that CM-1 exhibits a comparable activity (IC_{50} = 12.24 ± 0.69 µg/mL) to diclofenac, with each one exhibiting better activity compared to CM-2 (IC_{50} = 17.41 ± 0.63 µg/mL). Although epoxy-bearing fatty acids are promising targets against inflammatory diseases (McReynolds et al., 2020), the significant reduction in the anti-inflammatory activity of the epoxy-containing compound CM-2 in this study could be ascribed to its longer hydrocarbon chain compared to CM-1 (Chen et al., 2021).

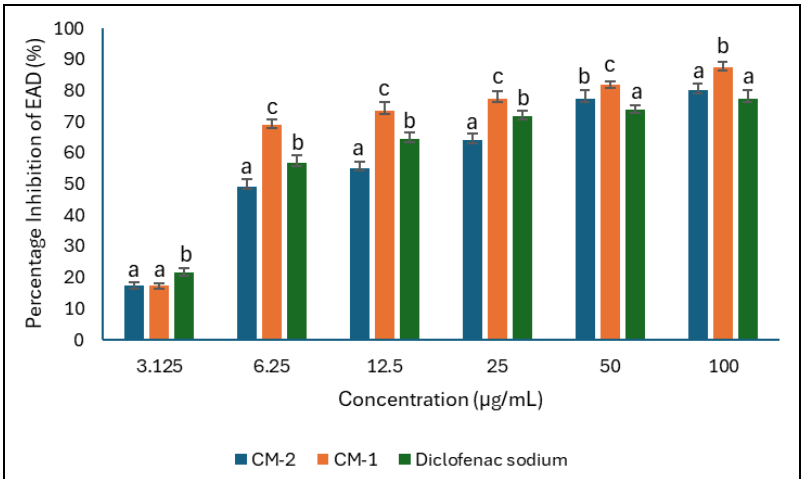


Figure 4. *In vitro* anti-inflammatory activity of ethyl margarate (CM-1) and nonadecanoic acid-2-ethoxy ethyl ester (CM-2) isolated from the leaves of *Cyperus marginatus*.

Table 4. *In vitro* anti-inflammatory activity of isolated compounds.

Isolated compounds	IC_{50} ± SEM (µg/mL)
Ethyl margarate	12.24 ± 0.69^{a}
Nonadecanoic acid-2-ethoxy ethyl ester	17.41 ± 0.63^{b}
Diclofenac (standard)	11.94 ± 1.37^{a}

Data are presented as mean ± SEM (n = 3). Values having different alphabets in superscript are considered significant at $p<0.05$, while those with the same alphabets are comparable ($p>0.05$).

In silico molecular docking

The molecular docking results showed exhilarating results against proteins. NOX is a membrane-bound ROS-producing enzyme. Superoxide is produced when an electron is transferred from one oxygen atom to another by the enzyme NOX. After converting from superoxide to hydrogen peroxide, CAT uses reduced GSH to catalyze the conversion into water further (Girima and Devendra, 2011). The results of the research showed that Ile67, Leu186, Ile189, Phe216, Phe215, Phe212, His209, His101, Leu68, Val71, Arg284, His210, Tyr280, Trp206, Arg287, Arg73, Phe202, Phe205, Arg198, Leu98, His101, Ser193, Trp106, Lys102, Ala105, Ile190, Ile108 formed the active site pocket in NOX2 (PDB ID 7U8G) (Fig. 5). The interaction of ethyl margarate with the hydrophobic interaction (Leu68, Arg73, His101, Ala105, Ile108, Leu186, Ile189, Trp206, His209, Phe212, Arg287), hydrogen bonds with residues (His210, Tyr280, Arg 284) and Pi-alkyl interactions (Ile67, Val71, Phe215, Phe216) of NOX2 protein displayed the binding energy score of -7.2 kcal/mol. Whereas hydrophobic interaction (Ile67, Leu68, Val71, Arg73, His101, Ala105, Ile108, Leu186, Ile190, His209, His210, Phe212, Phe216), hydrogen bonds (Trp206, Tyr280, Arg284, Arg287) and Pi-sigma interactions (Phe215), and alkyl interaction (Ile189) of NOX2 protein with the compound nonadecanoic acid 2-ethoxy ethyl ester returned a binding energy score of -6.7 kcal/mol. The standard L-ascorbic acid showed a binding energy score of -5.7 kcal/mol with hydrophobic interactions (His115, His119, Ala175, Ile182), hydrogen bond (Gly176, Gly179, Thr183, His222) (Table 5 and Fig. 6A-C). It is interesting to note that the two FAEs significantly inhibited ROS production, as shown in the *in-vitro* antioxidant assay, which is also supported by the *in silico* results.

The NF-κB protein and the native ligand produced the active site pocket (Fig. 7). Furthermore, ethyl margarate interacted with the hydrophobic interaction (Leu406, Gly407, Arg408, Val414, Lys429, Met469, Glu470, Leu472, Gly475, Ser476, Gln479, Asp519, Asn520, Cys533, Asp534), hydrogen bonds (Gly409) and alkyl interactions (Ala427, Leu471, Leu522) of the protein NF-κB, returning a binding energy score of -6.1 kcal/mol. On the other hand, nonadecanoic acid-2-ethoxy ethyl ester's interaction with NF-κB (hydrophobic interaction: Leu406, Gly407, Arg408, Gly409, Phe411, Val414, Ala427, Met469, Leu472, Gly475, Ser476, Gln479, Asp519, Asn520, Leu522, Cys533, Asp534, and hydrogen bonds: Ser410, Gly412) displayed an energy score of -6.0 kcal/mol.

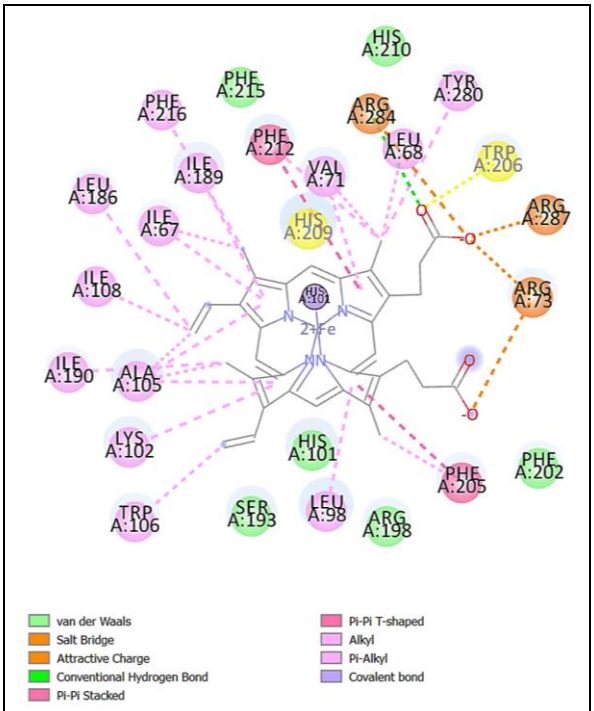


Figure 5. Amino acids formed the active site pocket in NOX2.

Table 5. The binding affinity of receptors (protein) with fatty acid esters from *C. marginatus* leaf.

Phytocompounds	Binding affinities (Kcal/mol)	
	NOX2 (7U8G)	NF-κB (4DN5)
Ethyl margarate	-7.2	-6.1
Nonadecanoic acid-2-ethoxy ethyl ester	-6.7	-6.0
L-Ascorbic acid (standard)	-5.7	---
Diclofenac (standard)	---	-5.9

However, the standard diclofenac is not far behind, as it showed -5.9 kcal/mol with the hydrophobic interactions (Gly407, Gly409, Lys429, Met469, Ser476, Asp519, Asn520), hydrogen bonds (Arg408, Cys533), Pi-alkyl (Leu406, Val414), Pi-anion (Asp534) and Pi-sigma (Leu522) interactions (Table 5 and Fig. 8A-C). As we know, inflammation is mostly caused by NF-κB. In addition, it controls the manufacture of cytokines and cell viability; it has occasionally been connected to cancer and autoimmune diseases. Therefore, inhibiting this protein might be a worthwhile goal for conditions linked to inflammation (Banerjee et al., 2022). We discovered that both the FAEs exhibited encouraging outcomes in terms of their anti-inflammatory activity *in vitro*, corroborating the *in silico* findings. Thus, ethyl margarate and nonadecanoic acid-2-ethoxy ethyl ester have been demonstrated through this study to be promising FAEs for reactive oxygen species (ROS) and inflammation-related conditions.

In silico analysis of physicochemical features and toxicity indices

The pharmacokinetics of pharmacological leads are estimated by assessing a substance's physicochemical properties (Kar et al., 2022b; Naidoo et al., 2021). We used Veber's rule (Veber et al., 2002) and Lipinski's rule of five (Lipinski et al., 2001) to assess the compounds' physicochemical characteristics. In order to determine the compounds' possible druggability in relation to the medications, their physicochemical characteristics were compared to those of the pertinent standard drugs, L-ascorbic acid and diclofenac. It was discovered that the physicochemical characteristics of the relevant phytochemicals, such as ethyl margarate and nonadecanoic acid-2-ethoxy ethyl ester, were completely consistent with Veber's rule and Lipinski's rule of five (RO5), indicating their significant drug-like potential (Table 6).

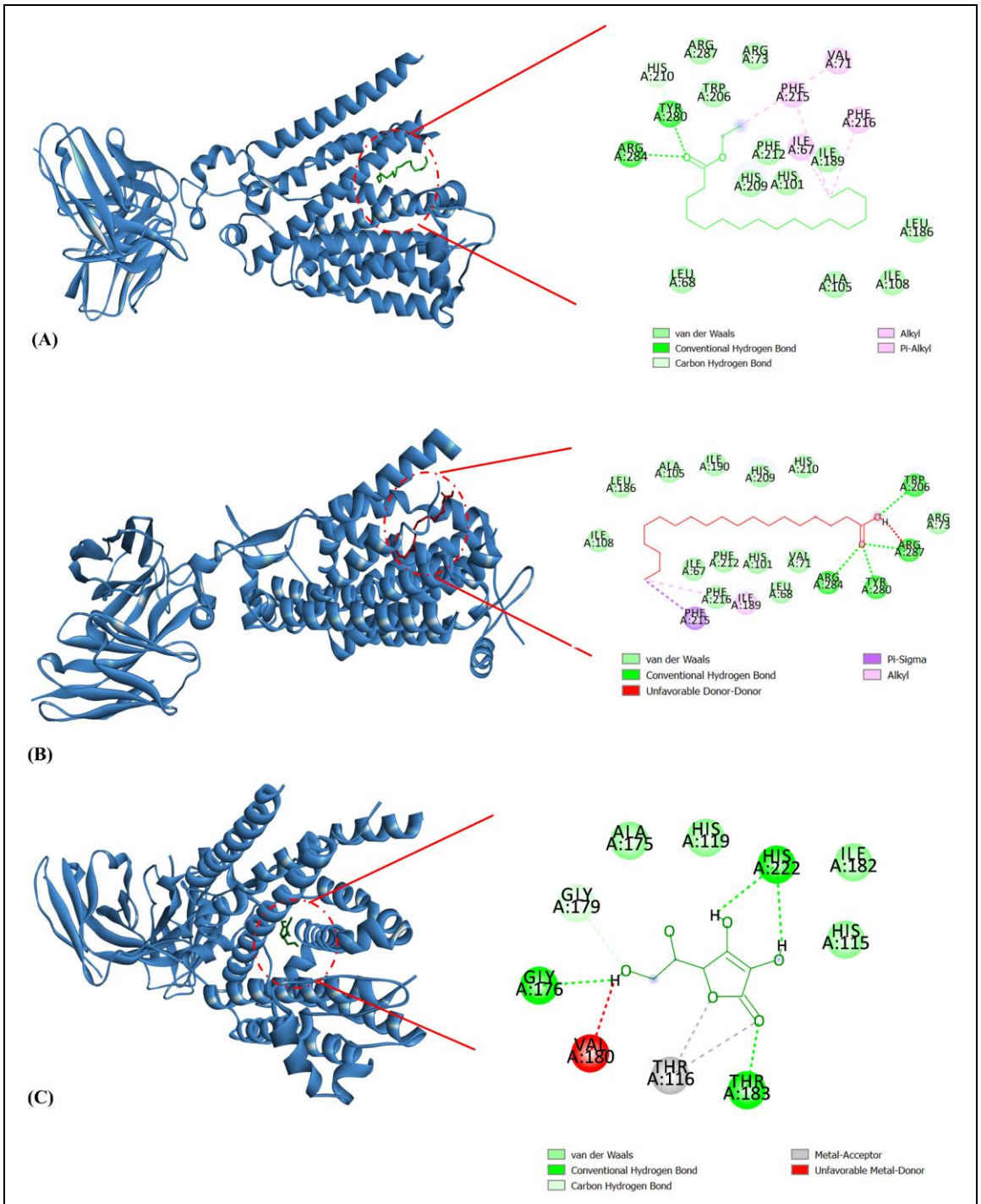


Figure 6. Molecular docking interactions of NOX2 with **(A)** ethyl margarate, **(B)** nonadecanoic acid-2-ethoxy ethyl ester, and **(C)** L-ascorbic acid.

The blue ribbon represents the NOX2 protein.

According to Wang et al. (2017), it has been suggested that *in silico* toxicity prediction and evaluation of potential treatment candidates may be important in the early phases of drug development. According to a thorough *in silico* toxicity evaluation, the substance ethyl margarate was found to be non-mutagenic, non-cytotoxic, non-hepatotoxic, and carcinogenic, whereas nonadecanoic acid-2-ethoxy ethyl ester was found to have the potential to be non-mutagenic, non-carcinogenic, non-cytotoxic, and non-hepatotoxic (Table 7). Finding compounds with structural alarms is a crucial screening step in the drug development process. The phrase "toxicophores" describes PAINS (panassay interference compounds), which are known to disrupt biological tests, interact with proteins and DNA, and, among other potentially harmful effects,

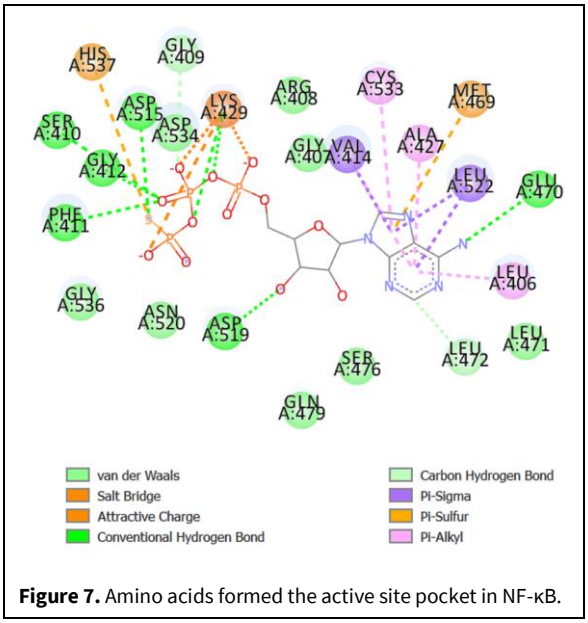


Figure 7. Amino acids formed the active site pocket in NF-κB.

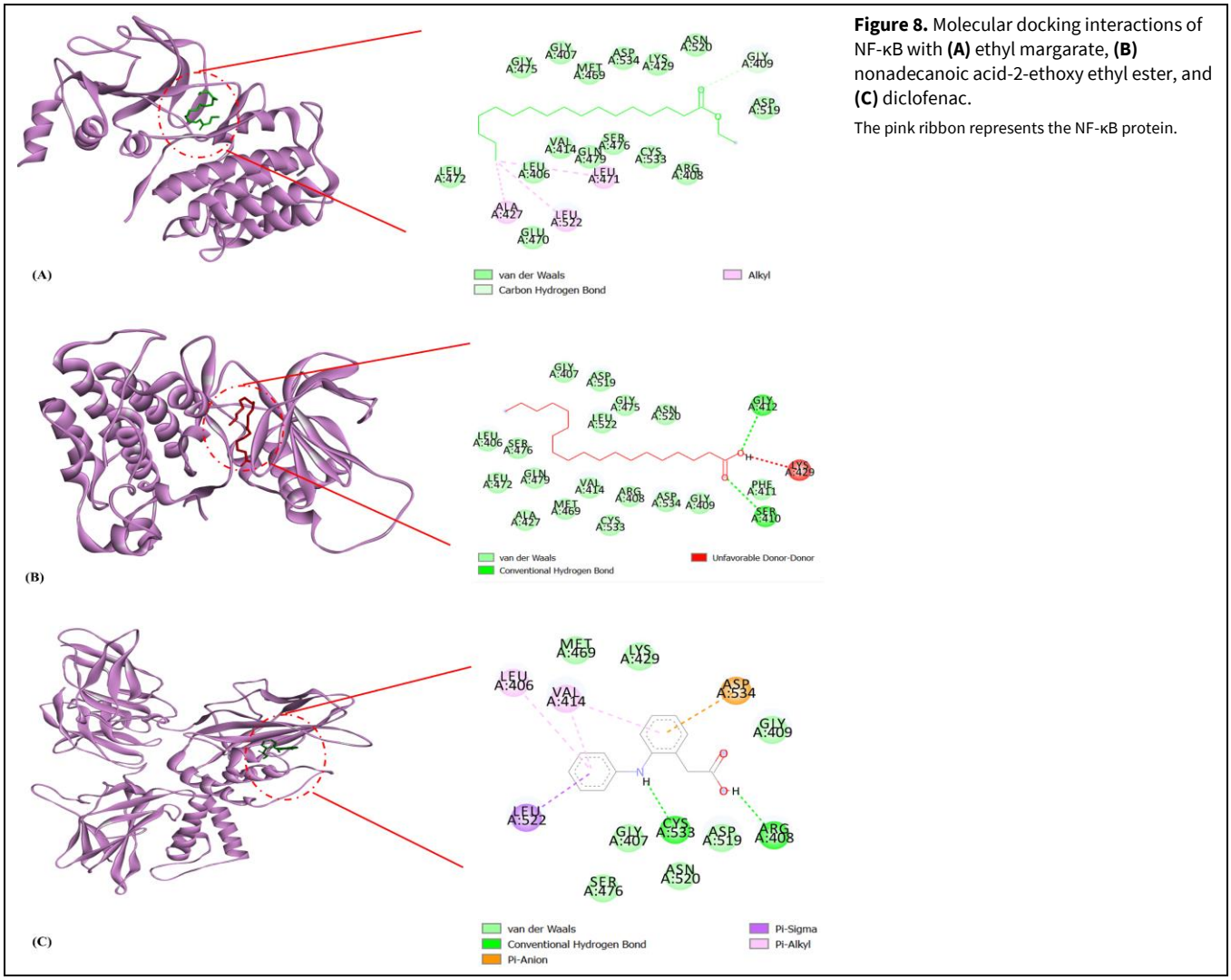


Figure 8. Molecular docking interactions of NF-κB with **(A)** ethyl margarate, **(B)** nonadecanoic acid-2-ethoxy ethyl ester, and **(C)** diclofenac.

The pink ribbon represents the NF-κB protein.

Table 6. Physicochemical properties of the phytochemicals isolated from *Cyperus marginatus* leaf extracts and their accordance with the rules of drug-likeness.

Physicochemical properties	Compound			
	Ethyl margarate	Nonadecanoic acid-2-ethoxy ethyl ester	L-ascorbic acid (standard)	Diclofenac (standard)
Molecular weight (Dalton)	298.50	298.50	176.12	296.15
Number of Hydrogen bond acceptor (HBA)	2	2	6	2
Number of Hydrogen bond donor (HBD)	0	1	4	2
No. of rotatable bonds	17	17	2	4
TPSA (Å^2)	26.30	37.30	107.22	49.33
log P	6.42	6.72	-1.41	4.44
In accordance with Lipinski's rule of Five (RO5)	Yes; 1 violation	Yes; 1 violation	Yes	Yes
In accordance with Veber's rule	No; 1 violation	No; 1 violation	Yes	Yes

Mol. Wt: Molecular weight; TPSA: Topological Polar Surface Area; log P: Logarithm of partial coefficient.

Table 7. *In silico* toxicity assessment of the concerned phytochemicals isolated from *Cyperus marginatus* leaf extracts.

Toxicity assessment	Compound			
	Ethyl margarate	Nonadecanoic acid-2-ethoxy ethyl ester	L-ascorbic acid (standard)	Diclofenac (standard)
Mutagenicity (AMES mutagenesis)	No	No	No	No
Cytotoxicity	No	No	No	No
Carcinogenicity	Yes	No	No	No
Hepatotoxicity	No	No	No	Yes
Medicinal Chemistry (PAINS)	0 alert	0 alert	0 alert	0 alert
P-glycoprotein inhibitor	Yes	No	No	No

PAINS: Pan-assay interference compounds.

result in hepatotoxicity, carcinogenicity, and CYP inhibition (Baell, 2010; Pouliot and Jeanmart, 2016). Since there were no PAINS structural alarms found, the relevant phytochemicals cleared the PAINS-related toxicity screening stage (Table 7). P-gp inhibitors can alter the pharmacokinetics of a medication, enhancing its distribution, absorption, and metabolism (Le et al., 2022). Based on *in silico* screening, ethyl margarate was the suitable P-gp inhibitor (Table 7). Thus, ethyl margarate, the relevant phytocompound demonstrated promising drug-like qualities and provided further prospects for *in vitro* and *in vivo* validation towards the development of effective therapies for reactive oxygen species (ROS) and inflammation-related diseases.

Molecular dynamics (MD) simulations

The compound ethyl margarate (heptadecanoic ethyl ester) had the best interaction with the NOX2 and NF-κB protein in terms of binding energy scores (Table 5). It was also predicted that the compound would be non-toxic. As a result, MD simulations of the respective protein-ligand complexes were run for 120 ns. The mean RMSD values of the ethyl margarate-NOX2 protein complexes (complex 1) and ethyl margarate-NF-κB protein (complex 2) were found to be 0.8 and 1.0 Å respectively. In contrast, the mean RMSF values were 1.7 and 1.5 Å for the corresponding complexes. The RMSD values of the C atoms in complexes 1 and 2 initially fluctuated, but after 95 and 102 ns, they stabilized and remained in equilibrium (Fig. 9A, C).

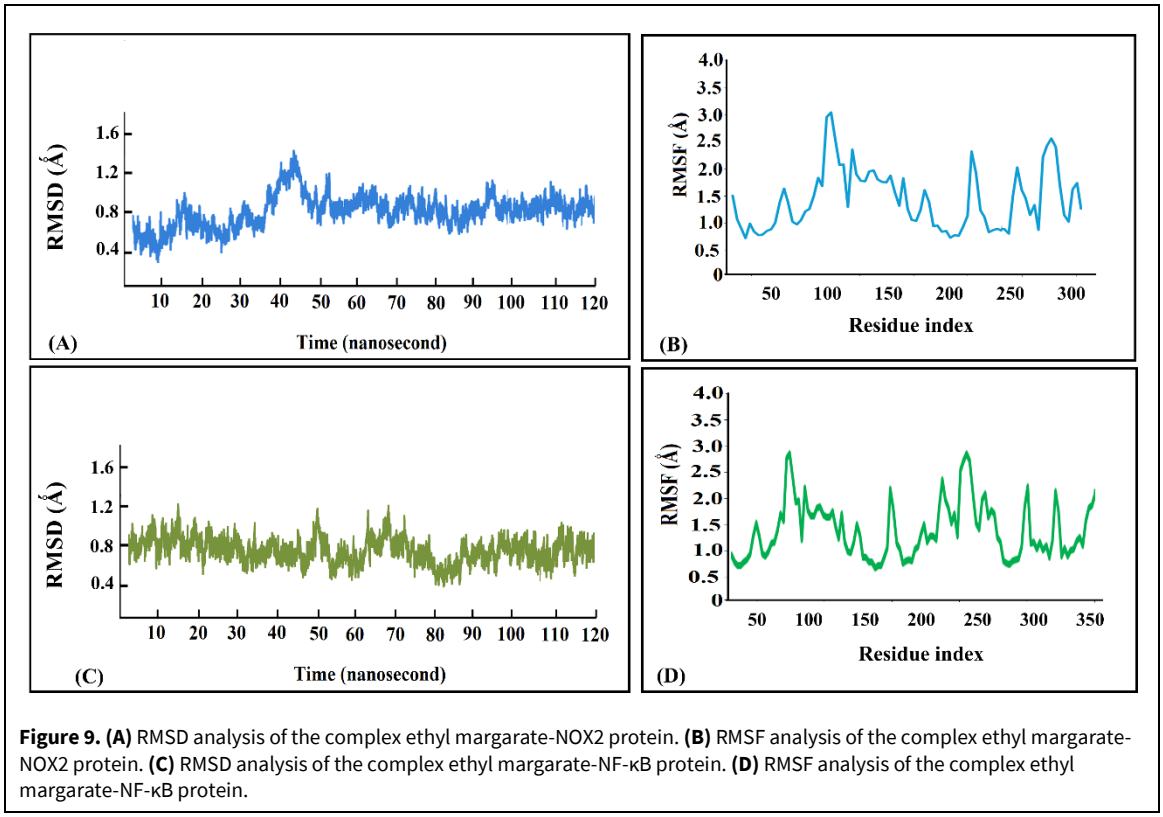


Figure 9. (A) RMSD analysis of the complex ethyl margarate-NOX2 protein. **(B)** RMSF analysis of the complex ethyl margarate-NOX2 protein. **(C)** RMSD analysis of the complex ethyl margarate-NF-κB protein. **(D)** RMSF analysis of the complex ethyl margarate-NF-κB protein.

In contrast, complexes 1 and 2's RMSF analysis revealed the fewest fluctuations and was generally stable over the course of the 120 ns MD simulations, reflecting the conformation stability of the corresponding complexes (Fig. 9B, D).

CONCLUSION

This study investigated the fatty acid composition and antioxidant properties of *Cyperus marginatus* leaves, focusing on compounds isolated from the dichloromethane extract. Two compounds, ethyl margarate, and nonadecanoic acid-2-ethoxy ethyl ester, were isolated and characterized from the plant for the first time. Ethyl margarate showed promising antioxidant and anti-inflammatory properties based on its considerable free radical (DPPH, NO, and Fe^{3+}) scavenging activity and inhibitory action against protein denaturation. These findings were corroborated in the *in silico* study, with ethyl margarate showing higher binding affinity to the NOX2 and NF-κB, which are proteins implicated in ROS and inflammation. The study findings contribute to the repository of chemical constituents of *C. marginatus* and highlight the biological potential of the FAEs, especially ethyl margarate, for possible cosmeceutical application.

Future studies could focus on investigating the bioavailability, bioactivity, and safety profiles of ethyl margarate and nonadecanoic acid-2-ethoxy ethyl ester in preclinical models. Moreover, exploring the synergistic effects of these compounds with other bioactive components of *C. marginatus* could provide a comprehensive understanding of the plant's medicinal potential. Additionally, clinical studies may be conducted to validate the antioxidant and anti-inflammatory properties of these compounds in humans. The identification of specific molecular targets and elucidation of underlying mechanisms of action could further enhance the establishment of these FAEs as therapeutic agents.

CONFLICT OF INTEREST

The authors declare no conflicts of interest.

ACKNOWLEDGMENTS

The authors are grateful to the Research Directorates of Walter Sisulu University (African Medicinal Flora and Fauna Niche Area and PDRFs) and NRF Rated Researcher Incentive for their financial support.

REFERENCES

Abraham MJ, Murtola T, Schulz R, Páll S, Smith JC, Hess B, Lindahl E (2015) GROMACS: High performance molecular simulations through multi-level parallelism from laptops to supercomputers. SoftwareX 1-2: 19–25. https://doi.org/10.1016/j.softx.2015.06.001

Abubakar MN, Majinda RR (2016) GC-MS analysis and preliminary antimicrobial activity of *Albizia adianthifolia* (Schumach) and *Pterocarpus angolensis* (DC). Medicines 3(1): 3. https://doi.org/10.3390/medicines3010003

Ait-Ouazzou A, Lorán S, Arakrak A, Laglaoui A, Rota C, Herrera A, Pagán R, Conchello P (2012) Evaluation of the chemical composition and antimicrobial activity of *Mentha pulegium*, *Juniperus phoenicea*, and *Cyperus longus* essential oils from Morocco. Food Res Int 45(1): 313–319. https://doi.org/10.1016/j.foodres.2011.09.004

Al-Snafi AE (2016) A review on *Cyperus rotundus* a potential medicinal plant. IOSR J Pharm 6(7): 32–48. http://dx.doi.org/10.9790/3013-06723248

Antwi AO, Obiri DD, Osafo N, Essel LB, Forkuo AD, Atobiga C (2018) Stigmasterol alleviates cutaneous allergic responses in rodents. BioMed Res Int 2018: 3984068. https://doi.org/10.1155/2018/3984068

Aparna V, Dileep KV, Mandal PK, Karthe P, Sadasivan C, Haridas M (2012) Anti-inflammatory property of n-hexadecanoic acid: Structural evidence and kinetic assessment. Chem Biol Drug Des 80(3): 434–439. https://doi.org/10.1111/j.1747-0285.2012.01418.x

Ayodele OA, Awotuya IO, Taiwo BJ, Osungunna OM, Vuyisa M, Kasim SL (2024) Two new triterpenoids from the leaf of *Ficus vogelii* and their antibacterial activities. Chem Afr 7: 63–70. https://doi.org/10.1007/s42250-023-00743-y

Baell JB (2010) Observations on screening-based research and some concerning trends in the literature. Future Med Chem 2(10): 1529–1546. https://doi.org/10.4155/fmc.10.237

Banerjee P, Eckert AO, Schrey AK, Preissner R (2018) ProTox-II: A webserver for the prediction of toxicity of chemicals. Nucleic Acids Res 46(W1): W257–W263. https://doi.org/10.1093/nar/gky318

Banerjee S, Kar P, Islam R, Naidoo D, Roy A, Sarkar I, Sen G, Saha T, Yasmin H, Sen A (2022) Synthesis of silver nanoparticles from secondary metabolites of star gooseberry fruit (*Phyllanthus acidus*) and their nephroprotective efficiency. S Afr J Bot 151 (Part A): 385–395. https://doi.org/10.1016/j.sajb.2022.10.021

Binkowski TA, Naghibzadeh S, Liang J (2003) CASTp: computed atlas of surface topography of proteins. Nucleic Acids Res 31(13): 3352–3355. https://doi.org/10.1093/nar/gkg512

Browning J, Gordon-gray K, Ward C (1999) Studies in Cyperaceae in southern Africa 36: *Cyperus marginatus*, a complex of three entities. S Afr J Bot 65(5-6): 374–381. https://doi.org/10.1016/S0254-6299(15)31025-5

Burdge GC, Calder PC (2015) Introduction to fatty acids and lipids. In: World Review of Nutrition and Dietetics. Intravenous Lipid Emulsions. Calder PC, Waitzberg DL, Koletzko BS (eds.). vol. 112. Karger AG, pp. 1–16. https://doi.org/10.1159/000365423

Chen U, She Y, Lei J, Wang D, Wu S, Men K (2021) Medium chain fatty acids: Extraction, isolation, purification, bioactive properties and application. IOP Conf Ser: Earth Environ Sci 705: 012013. https://doi.org/10.1088/1755-1315/705/1/012013

Daina A, Michielin O, Zoete V (2017) Swiss ADME: A free web tool to evaluate pharmacokinetics, drug-likeness and medicinal chemistry friendliness of small molecules. Sci Rep 7: 42717. https://doi.org/10.1038/srep42717

Dederen J, Chavan B, Rawlings A (2012) Emollients are more than sensory ingredients: The case of isostearyl isostearate. Int J Cosmetic Sci 34(6): 502–510. https://doi.org/10.1111/j.1468-2494.2012.00744.x

Demirpolat A, Akman F, Kazachenko AS (2022) An experimental and theoretical study on essential oil of *Aethionema sancakense*: Characterization, molecular properties and RDG analysis. Molecules 27(18): 6129. https://doi.org/10.3390/molecules27186129

Dharmadeva S, Galgamuwa L, Prasadinie C, Kumarasinghe N (2018) *In vitro* anti-inflammatory activity of *Ficus racemosa* L. bark using albumin denaturation method. AYU 39(4): 239–242. https://doi.org/10.4103/ayu.AYU_27_18

Dudley N (2008) Guidelines for applying protected area management categories. Gland, Switzerland: IUCN. 86 pp.

Elfiky AA, Azzam EB (2021) Novel guanosine derivatives against MERS CoV polymerase: An *in silico* perspective. J Biomol Struct Dyn 39(8): 2923–2931. https://doi.org/10.1080/07391102.2020.1758789

Enayatkhani M, Hasaniazad M, Faezi S, Guklani H, Davoodian P, Ahmadi N, Ahmadi K (2021) Reverse vaccinology approach to design a novel multi-epitope vaccine candidate against COVID-19: An *in silico* study. J Biomol Struct Dyn 39(8): 2857–2872. https://doi.org/10.1080/07391102.2020.1756411

Esperón-Rojas AA, Torres-Palacios C, Santos-Luna D, Baeza-Jiménez R, Cano-Sarmiento C, García HS (2018) A specific thin layer chromatography method for the Identification and separation of medium chain acylglycerols. J Oleo Sci 67(11): 1397–1403. https://doi.org/10.5650/jos.ess18081

Fiume MM, Bergfeld WF, Belsito DV, Hill RA, Klaassen CD, Liebler D, Marks JR, Shank RC, Slaga TJ, Snyder PW (2012) Safety assessment of stearyl heptanoate and related stearyl alkanoates as used in cosmetics. Int J Toxicol 31(suppl. 5): S141–S146. https://doi.org/10.1177/1091581812460408

Gamal M, Hani KM, Sameh ES, Sabrin IR (2015) A review: Compounds isolated from *Cyperus* species (Part I): Phenolics and nitrogenous. Int J Pharmacogn Phytochem 7(1): 51–67.

Gambo A, Da'u A (2014) Tiger nut (*Cyperus esculentus*): Composition, products, uses and health benefits - A review. Bayero J Pure Appl Sci 7(1): 56–61. http://dx.doi.org/10.4314/bajopas.v7i1.11

Girima N, Devendra KB (2011) Alleviation of lindane induced toxicity in testis of Swiss mice by combined treatment with vitamin C, vitamin E and alpha-lipoic acid. Indian J Exp Biol 49(3): 191–199.

Goyal A, Sharma A, Kaur J, Kumari S, Garg M, Sindhu RK, Rahman MH, Akhtar MF, Tagde P, Najda A, Banach-Albińska B, Masternak K, Alanazi IS, Mohamed HRH, El-Kott AF, Shah M, Germoush MO, Al-Malky HS, Abukhuwayjah SH, Altyar AE, Bungau SG, Abdel-Daim MM (2022) Bioactive-based cosmeceuticals: An update on emerging trends. Molecules 27(3): 828. https://doi.org/10.3390/molecules27030828

Gugsa T, Yaya EE (2018) Chemical constituents of the traditional skincare and fragrance nut, *Cyperus esculentus* (tigernut). Am Essen Oil Nat Prod 6(4): 4–12.

Han NR, Kim HM, Jeong HJ (2014) The β-sitosterol attenuates atopic dermatitis-like skin lesions through down-regulation of TSLP. Exp Biol Med 239(4): 454–464. https://doi.org/10.1177/1535370213520111

Kakarla L, Katragadda SB, Tiwari AK, Kotamraju KS, Madhusudana K, Kumar DA, Botlagunta M (2016) Free radical scavenging, α-glucosidase inhibitory and anti-inflammatory constituents from Indian sedges, *Cyperus scariosus* R. Br and *Cyperus rotundus* L. Pharmacogn Mag 12(47S): S488–S496. https://doi.org/10.4103/0973-1296.191467

Kar P, Kumar V, Vellingiri B, Sen A, Jaishee N, Anandraj A, Malhotra H, Bhattacharyya S, Mukhopadhyay S, Kinoshita M, Govindasamy V, Roy A, Naidoo D, Subramaniam MD (2022a) Anisotine and amarogentin as promising inhibitory candidates against SARS-CoV-2 proteins: A computational investigation. J Biomol Struct Dyn 40(10): 4532–4542. https://doi.org/10.1080/07391102.2020.1860133

Kar P, Sharma NR, Singh B, Sen A, Roy A (2021) Natural compounds from *Clerodendrum* spp. as possible therapeutic candidates against SARS-CoV-2: An *in silico* investigation. J

Biomol Struct Dyn 39(13): 4774–4785. https://doi.org/10.1080/07391102.2020.1780947

Kar P, Saleh-E-In MM, Jaishee N, Anandraj A, Kormuth E, Vellingiri B, Angione C, Rahman PKSM, Pillay S, Sen A, Naidoo D, Roy A, Choi YE (2022b) Computational profiling of natural compounds as promising inhibitors against the spike proteins of SARS-CoV-2 wild-type and the variants of concern, viral cell-entry process, and cytokine storm in COVID-19. J Cell Biochem 123(5): 964–986. https://doi.org/10.1002/jcb.30243

Kotze DC, Traynor CH (2011) Wetland plant species used for craft production in KwaZulu–Natal, South Africa: Ethnobotanical knowledge and environmental sustainability. Econ Bot 65: 271–282. https://doi.org/10.1007/s12231-011-9166-z

Lall N (2020) Aquatic plants of South Africa for pharmaceutical and cosmeceutical usage. WRC Report No. KV 349/15, Water Research Commission, 73 pp.

Le MT, Trinh DT, Ngo TD, Tran-Nguyen VK, Nguyen DN, Hoang T, Nguyen HM, Do TG, Mai TT, Tran TD, Thai KM (2022) Chalcone derivatives as potential inhibitors of P-glycoprotein and NorA: An *in silico* and *in vitro* study. Biomed Res Int 2022: 9982453. https://doi.org/10.1155/2022/9982453

Li C, Cheng X, Jia Q, Song H, Liu X, Wang K, Zhao C, Zhang Y, Ohlrogge J, Zhang M (2017) Investigation of plant species with identified seed oil fatty acids in Chinese literature and analysis of five unsurveyed Chinese endemic species. Front Plant Sci 8: 224. https://doi.org/10.3389/fpls.2017.00224

Lin TK, Zhong L, Santiago JL (2018) Anti-inflammatory and skin barrier repair effects of topical application of some plant oils. Int J Mol Sci 19(1): 70. https://doi.org/10.3390/ijms19010070

Lipinski CA, Lombardo F, Dominy BW, Feeney PJ (2001) Experimental and computational approaches to estimate solubility and permeability in drug discovery and development settings. Adv Drug Deliv Rev 46(1–3): 3–26. https://doi.org/10.1016/s0169-409x(00)00129-0

Liu J, Sudom A, Min X, Cao Z, Gao X, Ayres M, Lee F, Cao P, Johnstone S, Plotnikova O, Walker N (2012) Structure of the nuclear factor κB-inducing kinase (NIK) kinase domain reveals a constitutively active conformation. J Biol Chem 287(33): 27326–27334. https://doi.org/10.1074/jbc.M112.366658

Malan P (2003) Phytosociology of the wetland communities of cookes lake recreational area in Mmabatho, Northwest province, South Africa. S Afr J Bot 69(4): 555–562.

McReynolds C, Morisseau C, Wagner K, Hammock B (2020) Epoxy fatty acids are promising targets for the treatment of pain, cardiovascular disease and other indications characterized by mitochondrial dysfunction, endoplasmic stress and inflammation. In: Kihara Y (eds); Druggable Lipid Signaling Pathways. Advances in Experimental Medicine and Biology, vol. 1274. Springer, Cham, pp. 71–99. https://doi.org/10.1007/978-3-030-50621-6_5

Miya GM, Oriola AO, Payne B, Cuyler M, Lall N, Oyedeji AO (2023) Steroids and fatty acid esters from *Cyperus sexangularis* leaf and their antioxidant, anti-inflammatory and anti-elastase properties. Molecules 28(8): 3434. https://doi.org/10.3390/molecules28083434

Naidoo D, Roy A, Kar P, Mutanda T, Anandraj A (2021) Cyanobacterial metabolites as promising drug leads against the Mpro and PLpro of SARS-CoV-2: An *in silico* analysis. J Biomol Struct Dyn 39(16): 6218–6230. https://doi.org/10.1080/07391102.2020.1794972

Noreng S, Ota N, Sun Y, Ho H, Johnson M, Arthur CP, Schneider K, Lehoux I, Davies CW, Mortara K, Wong K, Seshasayee D, Masureel M, Payandeh J, Yi T, Koerber JT (2022) Structure of the core human NADPH oxidase NOX2. Nat Commun 13(1): 6079. https://doi.org/10.1038/s41467-022-33711-0

O'Boyle NM, Banck M, James CA, Morley C, Vandermeersch T, Hutchison GR (2011) Open Babel: An open chemical toolbox. J Cheminf 3: 33. https://doi.org/10.1186/1758-2946-3-33

Oderinde RA, Tairu OA (1988) Evaluation of the properties of yellow nutsedge (*Cyperus esculentus*) tuber oil. Food Chem 28(3): 233–237. https://doi.org/10.1016/0308-8146(88)90055-6

Oriola AO, Aladesanmi AJ, Idowu TO, Akinwumi FO, Obuotor EM, Idowu T, Oyedeji AO (2021) Ursane-type triterpenes, phenolics and phenolic derivatives from *Globimetula braunii* leaf. Molecules 26(21): 6528. https://doi.org/10.3390/molecules26216528

Oriola AO, Miya GM, Singh M, Oyedeji AO (2023) Flavonol glycosides from *Eugenia uniflora* leaves and their *in vitro* cytotoxicity, antioxidant and anti-inflammatory activities. Sci Pharm 91(3): 42. https://doi.org/10.3390/scipharm91030042

Pavia DL, Lampman GM, Kriz GS, Vyvyan JR (2013) Nuclear magnetic resonance spectroscopy part five: advanced NMR techniques. In: Introduction to spectroscopy. Boston, MA, USA: Thomson Learning Inc., pp. 511–576.

Pires DE, Blundell TL, Ascher DB (2015) pkCSM: Predicting small-molecule pharmacokinetic and toxicity properties using graph-based signatures. J Med Chem 58(9): 4066–4072. https://doi.org/10.1021/acs.jmedchem.5b00104

Platzer M, Kiese S, Tybussek T, Herfellner T, Schneider F, Schweiggert-Weisz U, Eisner P (2022) Radical scavenging mechanisms of phenolic compounds: A quantitative structure-property relationship (QSPR) study. Front Nutr 9: 882458. https://doi.org/10.3389/fnut.2022.882458

Pouliot M, Jeanmart S (2016) Pan assay interference compounds (PAINS) and other promiscuous compounds in antifungal research. J Med Chem 59(2): 497–503. https://doi.org/10.1021/acs.jmedchem.5b00361

Premathilaka R, Silva M (2016) Bioactive compounds and antioxidant activity of *Bunchosia armenica*. World J Pharm Pharm Sci 5(10): 1237–1247.

Rivera Casado NA, Montes Horcasitas MdC, Rodríguez Vázquez R, Esparza García FJ, Pérez Vargas J, Ariza Castolo A, Ferrera-Cerrato R, Gomez Guzman O, Calva Calva O (2015) The fatty acid profile analysis of *Cyperus laxus* used for phytoremediation of soils from aged oil spill-impacted sites revealed that this is a C18:3 plant species. PLoS One 10(10): e0140103. https://doi.org/10.1371/journal.pone.0140103

Sarker U, Rabbani MG, Oba S; Eldehna WM, Al-Rashood ST, Mostafa NM, Eldahshan OA (2022) Phytonutrients, colorant pigments, phytochemicals, and antioxidant potential of orphan leafy *Amaranthus* species. Molecules 27(9): 2899. https://doi.org/10.3390/molecules27092899

Schüttelkopf AW, van Aalten DM (2004) PRODRG: A tool for high throughput crystallography of protein-ligand complexes. Acta Crystallogr D Biol Crystallogr 60(8): 1355–1363. https://doi.org/10.1107/S0907444904011679

Schyman P, Liu R, Desai V, Wallqvist A (2017) vNN web server for ADMET predictions. Front Pharmacol 8: 889. https://doi.org/10.3389/fphar.2017.00889

Sharma SK, Singh AP (2011) Antimicrobial investigations on rhizomes of *Cyperus rotundus* Linn. Der Pharm Lett 3(3): 427–431.

Slobodianiuk L, Budniak L, Marchyshyn S, Ivasiuk I (2021) Fatty acids composition study of *Cyperus esculentus* L. Norwegian J Dev Intern Sci 53: 20–23. http://dx.doi.org/10.24412/3453-9875-2021-53-1-20-23

Srivastava RK, Singh A, Srivastava GP, Lehri A, Niranjan A, Tewari SK, Kumar K, Kumar S (2014) Chemical constituents and biological activities of promising aromatic plant nagarmotha (*Cyperus scariosus* R. Br.): A review. Proc Indian Natn Sci Acad

80(3): 525–536. http://dx.doi.org/10.16943/ptinsa/2014/v80i3/55127

Trott O, Olson AJ (2010) AutoDock Vina: Improving the speed and accuracy of docking with a new scoring function, efficient optimization, and multithreading. J Comput Chem 31(2): 455–461. https://doi.org/10.1002/jcc.21334

Umesh Kundu D, Selvaraj C, Singh SK, Dubey VK (2021) Identification of new anti-nCoV drug chemical compounds from Indian spices exploiting SARS-CoV-2 main protease as target. J Biomol Struct Dyn 39(9): 3428–3434. https://doi.org/10.1080/07391102.2020.1763202

Vadgama RN, Odaneth AA, Lali AM (2015) Green synthesis of isopropyl myristate in novel single phase medium part I: Batch optimization studies. Biotechnol Rep 8: 133–137. https://doi.org/10.1016/j.btre.2015.10.006

Veber DF, Johnson SR, Cheng HY, Smith BR, Ward KW, Kopple KD (2002) Molecular properties that influence the oral bioavailability of drug candidates. J Med Chem 45(12): 2615–2623. https://doi.org/10.1021/jm020017n

Wang YY, Li J, Wu ZR, Zhang B, Yang HB, Wang Q, Cai, YC, Liu GX, Li WH, Tang Y (2017) Insights into the molecular mechanisms of *Polygonum multiflorum* Thunb-induced liver injury: A computational systems toxicology approach. Acta Pharmacol Sin 38(5): 719–732. https://doi.org/10.1038/aps.2016.147

Yadav N, Singh AP, Rana AC, Kumar S, Kaur P, Singh J, Jangra A, Kumar D (2022) *Aesculus indica*: an updated review on its pharmacognosy, phytochemistry and pharmacological profile. Egypt J Basic Appl Sci 9(1): 125–135. https://doi.org/10.1080/2314808X.2022.2045455

Yoo JC, Han JM, Nam SK, Ko OH, Park CH, Kee KH, Sohng JK, Jo JS, Seong CN (2002) Characterization and cytotoxic activities of nonadecanoic acid produced by *Streptomyces scabiei* subsp. chosunensis M0137 (KCTC 9927). J Microbiol 40(4): 331–334.

AUTHOR CONTRIBUTION:

Contribution	Miya GM	Oriola AO	Kar P	Oyedeji AO
Concepts or ideas	x	x		x
Design		x	x	x
Definition of intellectual content		x	x	
Literature search		x	x	
Experimental studies		x	x	
Data acquisition	x	x	x	
Data analysis		x	x	
Statistical analysis		x	x	
Manuscript preparation	x	x	x	
Manuscript editing		x	x	
Manuscript review	x	x	x	x

Citation Format: Miya GM, Oriola AO, Kar P, Oyedeji AO (2025) Isolation and characterization of fatty acid esters from *Cyperus marginatus* Thunb. leaf, their *in vitro* biological and *in silico* molecular docking studies. J Pharm Pharmacogn Res 13(s1): S27–S46. https://doi.org/10.56499/jppres24.2109_13.s1.27

Publisher's Note: All claims expressed in this article are solely those of the authors and do not necessarily represent those of their affiliated organizations, or those of the publisher, the editors and the reviewers. Any product that may be evaluated in this article, or claim that may be made by its manufacturer, is not guaranteed or endorsed by the publisher.

Open Access: This article is distributed under the terms of the Creative Commons Attribution 4.0 International License (http://creativecommons.org/ licenses/by/4.0/), which permits use, duplication, adaptation, distribution and reproduction in any medium or format, as long as you give appropriate credit to the original author(s) and the source, provide a link to the Creative Commons license and indicate if changes were made.

Supplementary data

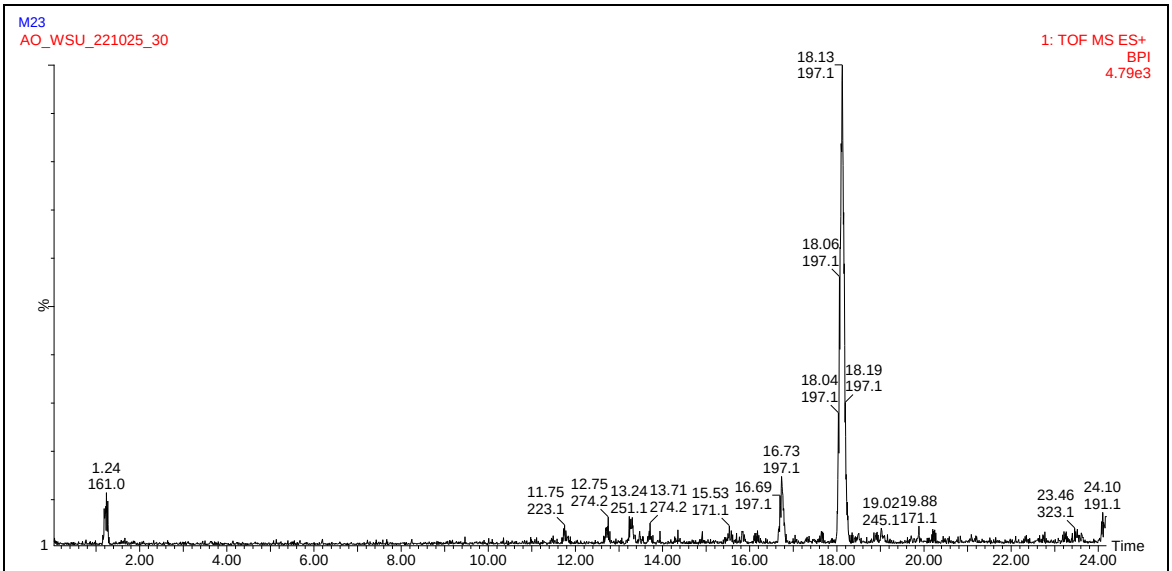


Figure S1. LC-MS Chromatogram of CM-1.

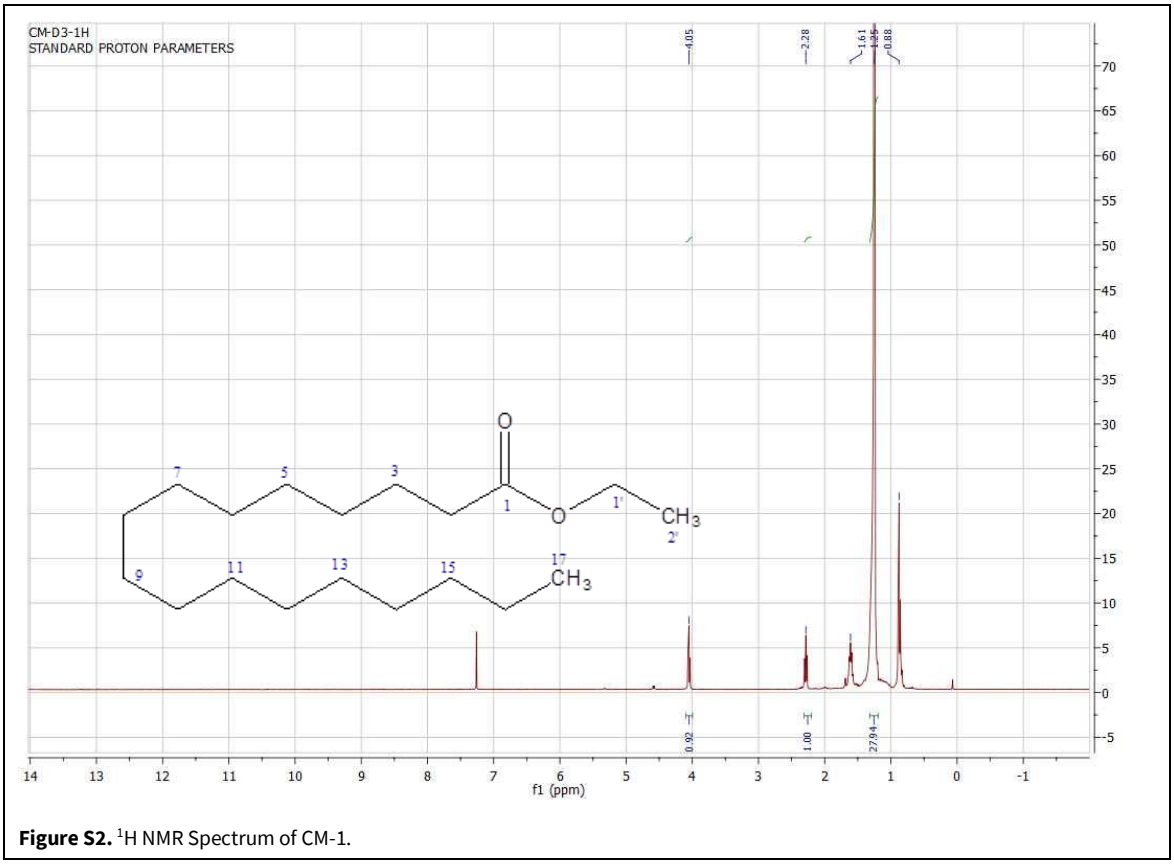


Figure S2. ^{1}H NMR Spectrum of CM-1.

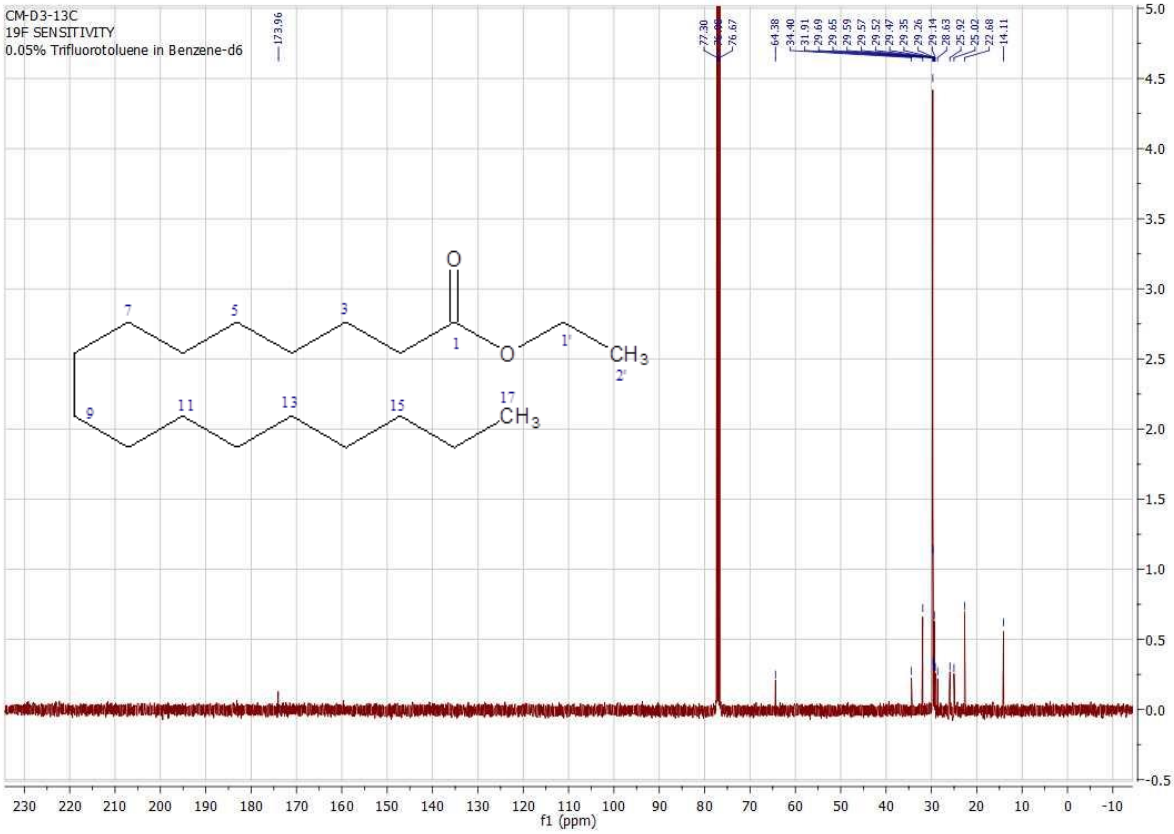


Figure S3. ^{13}C NMR Spectrum of CM-1.

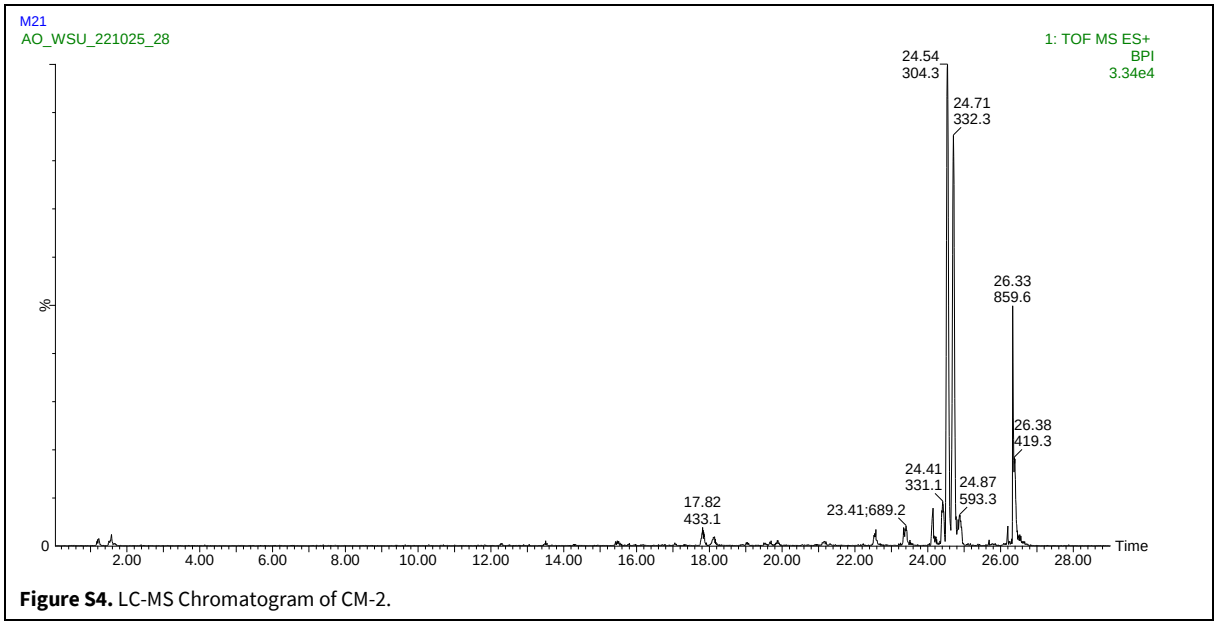


Figure S4. LC-MS Chromatogram of CM-2.

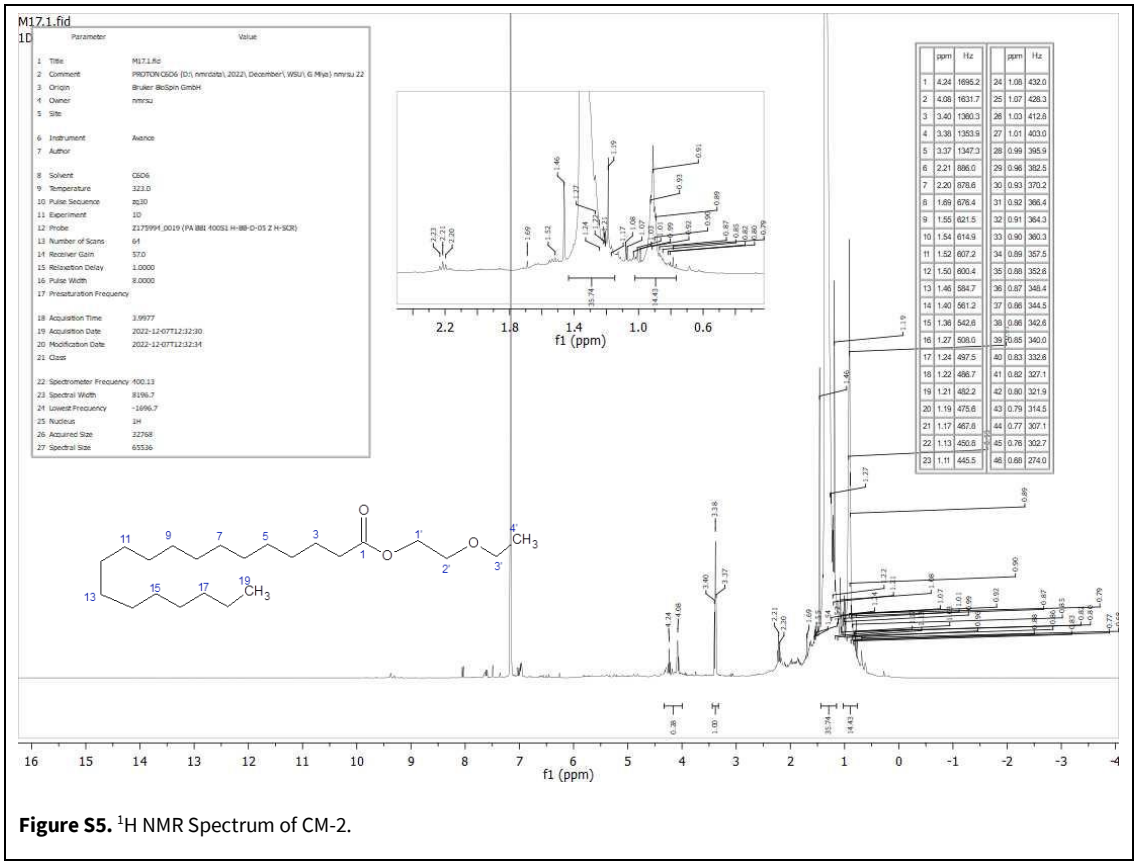


Figure S5. ^{1}H NMR Spectrum of CM-2.

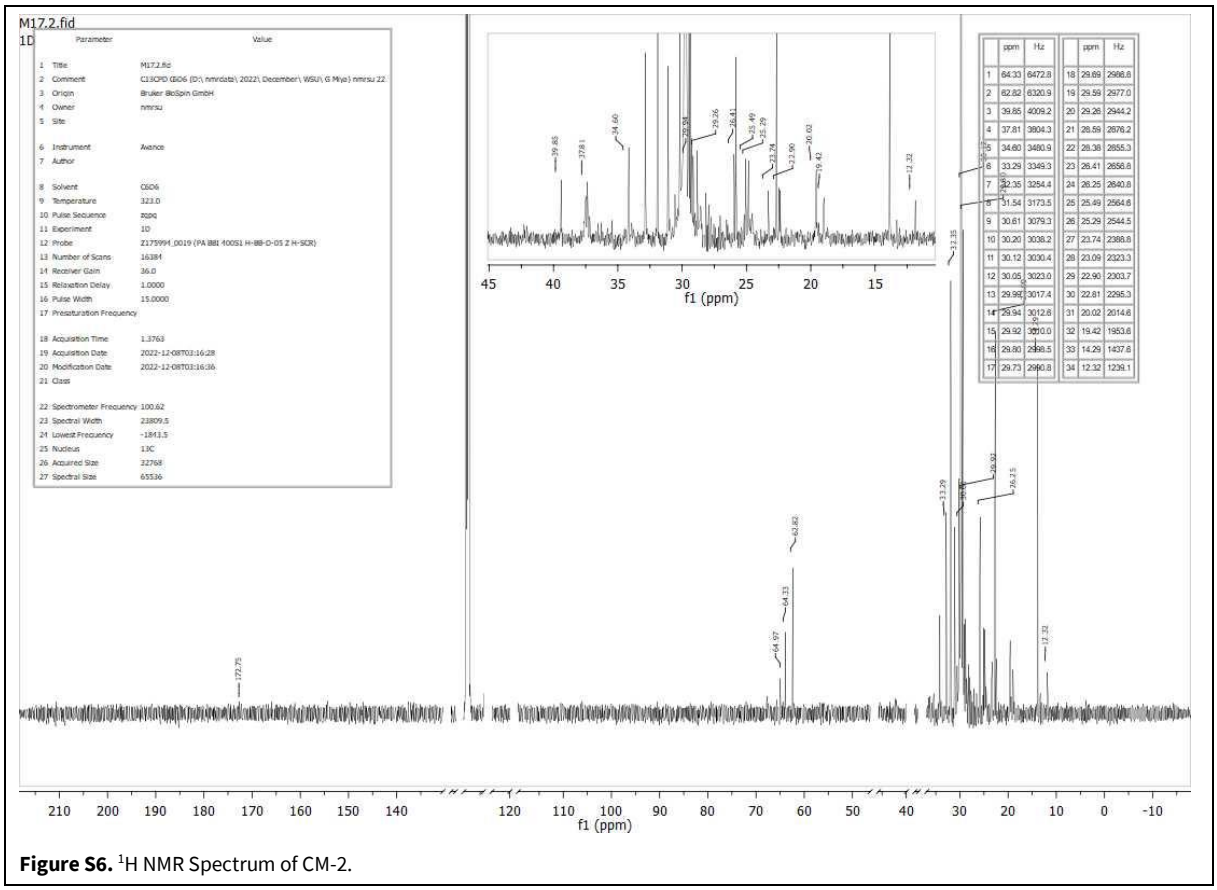


Figure S6. ^{1}H NMR Spectrum of CM-2.